Glass transition of polymers: Atomistic simulation versus experiments

Armand Soldera* and Noureddine Metatla
Department of Chemistry, Université de Sherbrooke, Sherbrooke, Québec, Canada J1K 2R1
(Received 29 April 2006; published 28 December 2006)

With experimental investigations and current theories, molecular modeling became an inevitable technique to study the perplexing phenomenon of glass transition. Among polymers, small variations in atomic interactions yield different values of the glass transition temperature, T_g. To reveal the influence of differences in the atomic functionality on the value of T_g, and thus to probe the molecular mechanisms responsible for this transition, atomistic simulations have to be undertaken. However, such simulations are argued not to accurately represent physically the glass transition due to the long relaxation times involved. Here we show the universality of the well-known Williams-Landel-Ferry equation for the experimental thermal dependence of polymer viscosities as demonstrated with atomistic simulations. Consequently, atomic aspects could be explicitly revealed. The contribution of atomistic simulation to the study of glass transition is thus confirmed. However, it has to be used complementarily with experiments and coarse-grained simulation to reveal the atomic aspects of current theories.

DOI: 10.1103/PhysRevE.74.061803 PACS number(s): 82.35.Lr, 64.70.Pf, 71.15.Pd

I. INTRODUCTION

A complete study of the glass transition phenomenon is a great scientific challenge [1]. It has to bridge many decades in both spatial and time scales [2]. No experiment can handle all the domain of investigation. The mode coupling theory (MCT) and landscape perspective brought additional viewpoints to understand the origin of this extraordinary slowdown of relaxation process [3,4]. To provide tests to these theoretical models, computer simulation is a prime candidate. However, molecular dynamics (MD) simulations with a full description of the atomic interactions through the use of force field involves an integration step of 10^{-15} s to remain on the surface of potential energy [5]. It corresponds in fact to the tenth of the C-H stretching mode vibration, the highest normal mode vibration found between atoms. Only short simulation durations can thus be accessed, and physical representation of the glass transition was evidently called into question [6]. By grouping atoms and adjusting the interaction potential, the integration step is increased, thereby revealing a greater domain of relaxation times [7,8]. Nevertheless, atomistic simulation (AS) could significantly contribute to a better understanding of the perplexing problem of the glass transition since it is able to explicitly reveal the effects of variations in atomic combinations [9]. However, there is no consensus in the literature concerning the value of T_gs stemming from AS: it ranges from a perfect agreement with the experimental data to clearly higher values. These differences to experimental data have different origins that stem from the AS of T_g itself; the number of configurations used to represent the phase space is low, cooling rate is too fast, and simulation cells are not equilibrated. The purpose of this article is to tackle these problems by clearly revealing the link between experimental and simulated data. This link is made by applying the well-established equation Williams-Landel-Ferry (WLF) to the AS of T_gs.

*Author to whom correspondence should be addressed. Email address: Armand.Soldera@USherbrooke.ca

The universal aspect of the viscous slowdown that appears at the glass transition is stated by the WLF equation [10,11]. It relates the time frame available by experiment to the temperature [10,11],

$$\log_{10} a_T = \log_{10} \frac{t}{t_g} = \frac{-C_1(T-T_g)}{C_2+T-T_g} \tag{1}$$

where $C_1=17.44$ and $C_2=51.6$ K for most of the experimental linear amorphous polymers, t/t_g corresponds to the ratio of cooling rates at the temperatures T and T_g [11], and a_T is called the reduced variable shift factor that tends to express the superimposing of the relaxation behavior at two different temperatures [10]. The validity of AS to depict the atomistic behavior occurring at the glass transition has to be confirmed by the relevance of the WLF equation. Correlations between simulated T_gs at different cooling rates have been corroborated using the Vogel-Fulcher-Tamman (VFT) equation, which is mathematically equivalent to the WLF equation [6,12]. In this study, VFT could not be used as the fitting equation, due to the limited number of points (three simulation cooling rates have been employed). However, evaluation of our data with simulated and experimental published results will be established on the basis of a comparative study of WLF parameters.

To verify the application of the WLF equation to the AS of polymers, it is necessary to consider a series of polymers whose T_gs are computed for different cooling rates. Polymers are actual good glass formers, and they are usually classified as fragile liquids, according to the denomination introduced by Angell [13,14]. Accordingly, the relaxation time domain probed by AS can closely approach the characteristic time of T_g (see, for instance, Fig. 2 of Ref. [3]). The polymers we studied are vinylic polymers, which can be differentiated from each other by small variations in atomic interaction combinations. These polymers are polyethylene (PE), isotactic and syndiotactic poly (methyl methacrylate) (*i*-PMMA and *s*-PMMA), isotactic and syndiotactic poly (α-methyl styrene) (*i*-PαMS and *s*-PαMS), polymethylacrylate (PMA), and polystyrene (PS). All these polymers possess the same

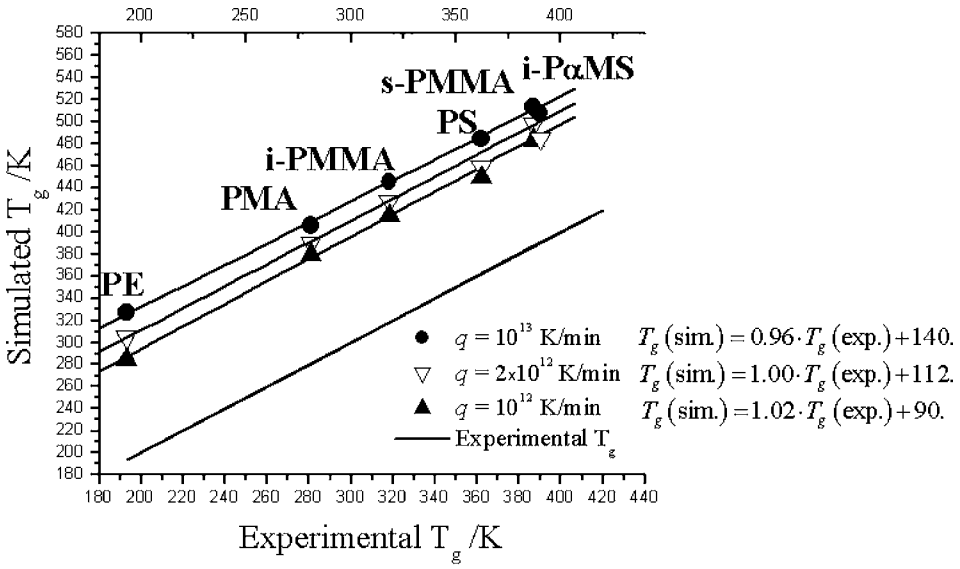

FIG. 1. Simulated T_gs of six polymers are reported versus experimental T_gs stemming from Table I, at three cooling rates: 1.2×10^{13}, 2.4×10^{12}, and 1.2×10^{12} K/min. The linear relationships between simulated and experimental T_gs obtained at these three cooling rates are also shown. The experimental equivalence line is also displayed.

backbone constituted by 200 carbon atoms. There is no side chain in PE, while an ester and phenyl groups are present in PMA and PMMA, and in PS and PαMS, respectively. The presence of an additional α-methyl group in PMMA and PαMS imparts to these polymers different T_gs according to the tacticity of their chain [15], while no significant difference in T_gs is observed between stereomers of PMA and PS. The aim of this study is to pursue investigation for a better description of the glass transition difference if atomic combinations among these polymers is accurately predicted by AS.

II. METHODOLOGY

The computation of T_g at different cooling rates has to be intimately associated with equilibrated initial systems. Actually, due to the long relaxation times of polymers, atomistic MD simulations inspect the region of phase space that is directly located near the initial portion [16]. The determination of the initial configurations is thus of primary importance since they dictate the final properties accessed by AS. According to statistical thermodynamics, a complete exploration of the phase space makes the time and ensemble averages of a property equal to the observable property [17]. This ergodic hypothesis is impossible to satisfy by simulations. An appropriate selection of starting states is needed [16,18]. The generation of the polymer chains was performed using the Theodorou-Suter and Meirovitch methods, which are based on self-avoiding walks implemented in the AMORPHOUS CELL code from Accelrys [16], although other codes exist [19–22]. In order to circumvent the major drawback of this method of generating relaxed configurations of a long chain [23], a specific procedure has been recently proposed [24]. 50 polymer chains are first generated, with only one chain inserted in a cell where the periodic boundary conditions are imposed. From these configurations, ten are selected for the determination of T_g according to two criteria. This choice is made in order to select the right portion of the configurational space. Configurations with a value of the radius of gyration, R_g, different from experimental data are removed. Also, an energy criterion has to be considered in order to eliminate the configurations with the highest energy. It is then argued that ten configurations stand for the description of the configurational space.

At this stage, determination of the T_g yields inaccurate values. Usually, a relaxation procedure based on simulated annealing is carried out: the system is heated to high temperatures, and then gently cooled down in order to eliminate excess entropy. We then carried out an additional optimization procedure: uniform hydrostatic compression [25] is undertaken until an energy minimum is reached [24]. The second generation force field from Accelrys, COMPASS, is used since it accurately represents nonbond interactions in the solid phase [26]. The densities corresponding to the minimum of energy are reported in Table I. An excellent agreement between experimental and simulated densities is observed for all the polymers considered in this work,

TABLE I. Comparison of simulated and experimental densities measured at 284 K for PE and at 298 K for *i*-PMMA, *s*-PMMA, PE, PS, *i*-PαMS, and *s*-PαMS, simulated T_gs at the three cooling rates (1, 2, and 3 for 1.2×10^{13}, 2.4×10^{12}, and 1.2×10^{12} K/min, respectively) and experimental T_gs.

Polymer	ρ_{sim} (g/cm^{-3})	$\rho_{expt.}$ (g/cm^{-3})	$T_g^{(1)}$ (K)	$T_g^{(2)}$ (K)	$T_g^{(3)}$ (K)	$T_g^{(expt.)}$ (K)
PMA	1.25±0.02	1.23[a]	406±4	390±4	380±3	280[b]
i-PMMA	1.186±0.004	1.188[c]	445±6	428±4	415±3	318[d]
s-PMMA	1.149±0.007	1.188[c]	513±7	498±4	483±3	387[d]
PE	0.907±0.005	0.86[e]	327±3	305±2	285±2	194
PS	1.078±0.011	1.062[f]	484±5	459±4	449±3	362[g]
i-PαMS	1.066±0.012	1.073[h]	508±6	485±5		390[h]
s-PαMS	1.031±0.011	1.073[h]	588±6	564±6		?

[a]Reference [41].
[b]Reference [42].
[c]Reference [43].
[d]Reference [44].
[e]Reference [45].
[f]Reference [35].
[g]Reference [11].
[h]Reference [46].

thereby revealing the accuracy of the procedure. AS of the polymer glass transition can then be performed: the configurational space is assumed to be correctly explored, and initial configurations are located in a potential well. In the determination of T_g, the first generation AMBER/OPLS force field is used since it requires less computer time than with the second generation force field. All MD simulations have been carried out in the NPT ensemble (i.e., constant number of particles, pressure and temperature), using the DL POLY code [27]. The integration has been performed using the Verlet-leapfrog integration algorithm with a 1 fs integration time step. During MD simulations, the Berendsen thermostat and barostat were considered to keep the system at prescribed temperatures and pressures [28]. The nonbonded interactions have been computed using the Ewald summation; a nonbond cutoff of 10 Å was selected. All the details of the simulation can be found in a recent publication [24].

The dilatometric technique is currently employed to determine the T_g experimentally. As the system cools down, the specific volume, i.e., the inverse density, is reported for different temperatures. The departure from a linear relationship between the specific volume and the temperature yields the value of the T_g which corresponds to the transition from the rubbery to the vitreous phases. This procedure is applied to AS in order to get the simulated T_g [29]. After heating the system to 800 K, it is cooled to 240 K by 20 K steps. How long the system remains at one temperature determines the cooling rate. This procedure is similar to the experiments performed by Kovacs, who demonstrated the influence of the time to reach an equilibrated volume in order to determine the T_g [30]. Nevertheless, due to the very low MD duration time, the ratio of the MD times and 20 K is considered as cooling rate. Thus, three cooling rates, q, have been used: 1.2×10^{13} (20 K/100 ps), 2.4×10^{12} (20 K/500 ps), and 1.2×10^{12} K/min (20 K/1,000 ps). These numerical cooling rates have to be compared to the experimental 10 K/min cooling rate. Glass transitions are observed due to the high cooling rates. Moreover, another heating-cooling process leads to the same T_g, revealing that the employed procedure, simulated annealing and hydrostatic compression, determines accurate and reproductive values of T_gs.

III. RESULTS AND DISCUSSION

The simulated $T_g s$ have to be compared to the experimental T_gs. However, different factors affect these latter values for a polymer: kinetic, type of experiment, molecular weight, etc. [31] To compensate for this problem, we employed the same procedure: experimental T_g values stemmed from the use of the empirical Fox-Flory equation [11,32] that relates the T_g to the molecular weight of the polymer. Table I presents the experimental T_gs stemming from the experimental Fox-Flory equation. The references are annotated therein, and the T_gs simulated at the three cooling rates are shown. Despite small standard deviations in the simulated T_gs, clear discrepancies with experimental T_g values are observed in Table I. However, as reported in Fig. 1, simulated

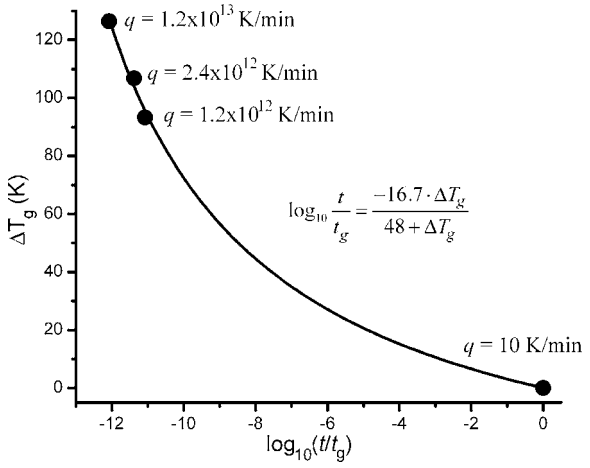

FIG. 2. Variation of the average value for *i*-PMMA, *s*-PMMA, PE, PS, *i*-PαMS and *s*-PαMS, of $\Delta T_g = T_{g(\text{sim.})} - T_{g(\text{expt.})}$ with respect to $\log_{10}(t/t_g)$. The fitting curve of the WLF equation is also shown.

$T_g s$ exhibit clear and unambiguous linear relationships with experimental T_gs. Such linear behavior has been outlined by Boyd's group [33]. In their studies, a direct proportional relationship between simulated and experimental T_gs has been established. Using the approach exposed in this text, the slope of the linear relationship between both T_gs is also approaching unity for the three cooling rates. The difference lies in the variation of the ordinate at the origin which clearly depends on q: it decreases as the cooling rate decreases, thus coming close to experimental value. It actually corresponds to the difference between simulated and experimental T_gs: $\Delta T_g = T_{g(\text{sim.})} - T_{g(\text{expt.})}$. This difference can be extracted from the WLF equation (1) by rearranging it, as follows:

$$\Delta T_g = \frac{-C_2 \log_{10} \dfrac{t_{g(\text{sim.})}}{t_{g(\text{expt.})}}}{C_1 + \log_{10} \dfrac{t_{g(\text{sim.})}}{t_{g(\text{expt.})}}}. \tag{2}$$

This equation expresses the fact that as the time frame $t_{g(\text{sim.})}/t_{g(\text{expt.})}$ decreases (i.e., as the cooling rate increases), so does T_g. Figure 2 reports average value performed on all polymers, i.e., PE, PMA, *i*-PMMA, *s*-PMMA, PS, *i*-PαMS, and *s*-PαMS, of ΔT_g with respect to $\log_{10}(t_{g(\text{sim.})}/t_{g(\text{expt.})})$, and C_1 and C_2 can thus be determined by fitting Eq. (2): $C_1 = 16.7 \pm 0.9$, and $C_2 = 48 \pm 8$ K. It has to be pointed out that the fit has been performed by considering simulated and experimental values; a very long range of data is thus described. However, sensitivity of C_1 and C_2 on the shape of the curve in simulation time range has to be examined. Actually, variations of C_2 do not greatly affect the shape of the curve. Conversely, modifications of C_1, which is related to the free volume [10], yields great changes. Consequently, since these values remarkably approach the "universal constant" values [11], the glass transition behavior is well depicted by atomistic simulation. However, different values of

TABLE II. Comparison of simulated and experimental WLF fitting parameters, C_1 and C_2.

Polymer	C_1	C_2 (K)	$C_1^{(expt.)}$	$C_2^{(expt.)}$ (K)
PMA	19.0	72.8	16.7[a]	60[a]
i-PMMA	17.7	59.3	9.3[b,c]	32.5[c]
			8.9[b,d]	23[d]
s-PMMA	17.7	59.6	11.3[d,e]	51[d]
			14.3[f,g]	63.1[g]
			34.0[h,i]	80[i]
PE	15.6	38.9	12.7[j,k]	63.3[k]
PS	15.7	36.2	13.3[i]	47.5[i]
			13.5[l]	28.9[l]

[a]Reference [47].
[b]*i*-PMMA.
[c]Reference [48].
[d]Reference [49].
[e]*s*-PMMA.
[f]Conventional PMMA.
[g]Reference [50].
[h]*a*-PMMA.
[i]Reference [10].
[j]Solution-chlorinated polyethylene.
[k]Reference [51].
[l]Reference [52].

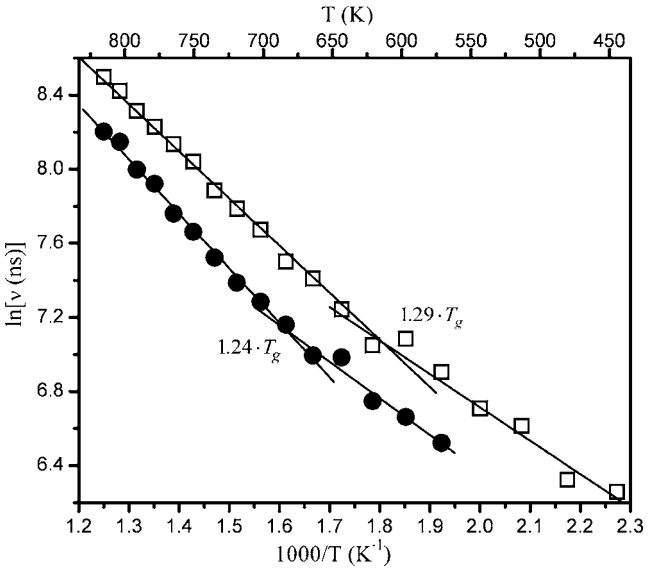

FIG. 3. Neperian logarithm of the number of backbone rotation between rotameric states during 1 ns, for *i*-PMMA (□) and *s*-PMMA (●) with respect to the inverse of the temperature.

C_1 and C_2 are obtained for each polymer as it is reported in Table II. A more detailed comparison was then undertaken in order to consider published data of PS and PMMA polymers in order to ensure the accuracy of the procedure.

From a simulation viewpoint, the VFT equation is employed instead of the WLF equation since no knowledge of experimental T_g is needed. Its current expression is [6,12,34]

$$T_g(q) = T_o - \frac{B}{\log_{10}(Aq)}, \tag{3}$$

where B, A, and T_o are the adjustable parameters, and q is the cooling rate. Consequently, T_o is the T_g at infinite slow cooling rate. This equation could not be applied in our approach, since only three different q have been used. However, this limitation could be compensated by comparing C_1 and C_2 parameters to published simulated data. A very interesting simulation study has been carried out by Lyulin *et al.* on the T_g of PS using the VFT equation [12]. The polymer was of 80 repeat units length yielding an experimental T_g of 359 K if the Fox-Flory equation is used [35]. The WLF parameters thus obtained are 14.0 and 8.0 K for C_1 and C_2, respectively. Compared to our simulated data, they are found in the same order. A slight discrepancy is found for C_2 that is compensated by a more accurate value of C_1 (Table II). Since the two simulations have been carried out separately, and yield relatively good agreement with experiment, it confirms that the proposed approach exposed in this text is accurate.

It has to be pointed out that different experimental values of the WLF parameters are found in the literature for each polymer (Table II). A well-documented study has been carried out by Fuchs *et al.* on the determination of these parameters for PMMA of different chain tacticities [36]. One measurement considered T_g as the reference temperature. Ensuing results can thus be compared to our simulations whose reference temperature is also T_g. The values of C_1 and C_2 for PMMA of different chain tacticities range from 11.9 to 21.1 and 58 to 114 K, respectively [36]. Simulated data for PMMA chain tacticities are included in these domains. From a comparative experimental viewpoint, such results confirm the accuracy of the proposed approach. More significantly, simulated C_1 and C_2 are found equivalent for both PMMA configurations in perfect agreement with experimental data [36] and the free volume theory [7]. In fact, for both PMMA chain tacticities, at the glass transition, the chain mobility is achieved for the same fraction of free volume. It is the C_1 parameter that actually takes into account this fraction. The proposed procedure clearly reproduces WLF parameters and the intimate difference or similarity between polymers with different chain tacticities.

IV. CONCLUSION

Despite the fact that the cooling rates employed in AS are many orders of magnitude larger than in the experiments, we clearly established the applicability of the WLF equation. The WLF fit indicates the reliable depiction of the glass transition by AS. The focused selection of the configurational space and the relaxation procedure circumvent AS drawbacks. AS can thus monitor more exotic correlations that are not easily accessible by experiments. Our results pave the way for numerous studies. For instance, for PMMA where the different configurations yield a difference in T_gs but not in the WLF parameters, the number of transitions between rotameric states, i.e., trans or gauche states, for the two stereomers of PMMA is reported versus the inverse of the temperature in Fig. 3. The Arrhenius behavior associated with the number of transitions inside the backbone is explained by

the existence of cooperatively rearranging regions (CRR) introduced by Adam and Gibbs [37], since one backbone rotation automatically comes with another non-neighboring backbone rotation. Moreover, a neat rupture in the slope is observed; it happens at 1.29 and 1.24 times T_g for *i*-PMMA and *s*-PMMA, respectively. These temperatures are in the same range as the crossover temperature predicted by MCT. Accordingly, physical mechanisms can be revealed by AS. Moreover, the linear relationship obtained between experimental and simulated T_gs (Fig. 1) can be used as a predictive tool. In fact, based on our numerical studies the T_g of *s*-PαMS is estimated to be roughly 200 °C for a mass of 11 800 g/mol. No Fox-Flory equation for *s*-PαMS has been found in the literature [38].

We showed that AS accurately depicts the glass transition since a correlation with experimental data has been clearly established. AS is thus a complementary tool to coarse-grained simulations and experiments to study this intricate phenomenon. By probing atomic interactions, it injects a valuable atomic viewpoint in present theories and will make beneficial contributions to glass transition related problems, such as the polymer behavior at the interface [39,40].

ACKNOWLEDGMENTS

The present work was supported by the Natural Sciences and Engineering Research Council (NSERC) of Canada and the Université de Sherbrooke. Computations have been made available thanks to the Canadian Fund Innovation (CFI), the Fonds Québécois de la Recherche sur la Nature et les Technologies (FQRNT), and Réseau Québécois de Calcul Haute Performance (RQCHP). We wish also thank Prof. S. Lacelle for fruitful scientific discussions.

[1] E. Donth, *The Glass Transition* (Springer-Verlag, New York, 2001).
[2] M. D. Ediger, C. A. Angell, and S. R. Nagel, J. Phys. Chem. **100**, 13200 (1996).
[3] P. G. Debenedetti and F. H. Stillinger, Nature **410**, 259 (2001).
[4] L. Berthier, G. Biroli, J.-P. Bouchaud, L. Cipelletti, D. El Masri, D. L'Hôte, F. Ladieu, and M. Pierno, Science **310**, 1797 (2005).
[5] F. Yonezawa, Science **260**, 635 (1993).
[6] J. Buchholz, W. Paul, and K. Binder, J. Chem. Phys. **117**, 7364 (2002).
[7] K. Binder, J. Baschnagel, and W. Paul, Prog. Polym. Sci. **28**, 115 (2003).
[8] K. Binder, J. Horbach, W. Kob, W. Paul, and F. Varnik, J. Phys.: Condens. Matter **16**, S429 (2004).
[9] A. Soldera, Macromol. Symp. **133**, 21 (1998).
[10] J. D. Ferry, *Viscoelastic Properties of Polymers* (Wiley, New York, 1970), p. 671.
[11] L. H. Sperling, *Introduction to Physical Polymer Science* (John Wiley & Sons, Ins., New York, 1992).
[12] A. V. Lyulin, N. K. Balabaev, and M. A. J. Michels, Macromolecules **36**, 8574 (2003).
[13] C. A. Angell, J. Non-Cryst. Solids **102**, 205 (1988).
[14] T. Scopigno, G. Ruocco, F. Sette, and G. Monaco, Science **302**, 849 (2003).
[15] F. E. Karasz and W. J. MacKnight, Macromolecules **1**, 537 (1968).
[16] D. N. Theodorou and U. W. Suter, Macromolecules **18**, 1467 (1985).
[17] F. Reif, *Fundamentals of Statistical and Thermal Physics* (McGraw Hill, Boston, 1965).
[18] D. J. Tildesley, Faraday Discuss. **100**, C29 (1995).
[19] S. Queyroy, S. Neyertz, D. Brown, and F. Müller-Plathe, Macromolecules **37**, 7338 (2004).
[20] P. Robyr, M. Muller, and U. W. Suter, Macromolecules **32**, 8681 (1999).
[21] E. Zervopoulou, V. G. Mavrantzas, and D. N. Theodorou, J. Chem. Phys. **115**, 2860 (2001).
[22] A. Uhlherr, V. G. Mavrantzas, M. Doxastakis, and D. N. Thodoru, Macromolecules **34**, 8554 (2001).
[23] V. G. Mavrantzas and D. N. Theodorou, Macromolecules **31**, 6310 (1998).
[24] N. Metatla and A. Soldera, Mol. Simul. **32**, 1187 (2006).
[25] D. N. Theodorou and U. W. Suter, Macromolecules **19**, 139 (1986).
[26] H. Sun, J. Phys. Chem. B **102**, 7338 (1998).
[27] W. Smith and T. R. Forrester, J. Mol. Graphics **14**, 136 (1996).
[28] H. J. C. Berendsen, J. P. M. Postma, W. F. Van Gunsteren, A. DiNola, and J. R. Haak, J. Chem. Phys. **81**, 3684 (1984).
[29] R. J. Roe, J. Non-Cryst. Solids **235-237**, 308 (1998).
[30] A. J. Kovacs, Adv. Polym. Sci. **3**, 394 (1964).
[31] D. J. Plazek and K. L. Ngai, in *Physical Properties of Polymers Handbook*, edited by J. E. Mark (A.I.P., Woodbury, NY, 1996), p. 139.
[32] T. G. Fox and P. J. Flory, J. Appl. Phys. **21**, 581 (1950).
[33] J. Han, R. H. Gee, and R. H. Boyd, Macromolecules **27**, 7781 (1994).
[34] R. Bruning and K. Samwer, Phys. Rev. B **46**, 11318 (1992).
[35] M. Mosiewicki, J. Borrajo, and M. I. Aranguren, Polym. Int. **54**, 829 (2005).
[36] K. Fuchs, C. Friedrich, and J. Weese, Macromolecules **29**, 5893 (1996).
[37] G. Adam and J. H. Gibbs, J. Chem. Phys. **43**, 139 (1965).
[38] J. M. G. Gowie and P. M. Toporowski, Eur. Polym. J. **4**, 621 (1968).
[39] Y. Grohens, L. Hamon, G. Reiter, A. Soldera, and A. Holl, Eur. Phys. J. E **8**, 217 (2002).
[40] R. D. Priestley, C. J. Ellison, L. J. Broadbelt, and J. M. Torkelson, Science **309**, 456 (2005).
[41] P. Zoller and D. J. Walsh, *Standard Pressure-Volume-Temperature Data for Polymers* (Technomic, Lancaster, 1995).
[42] X. Y. Lu and B. Z. Jiang, Polymer **32**, 471 (1991).
[43] W. G. Gall and N. G. McMrum, J. Polym. Sci. **50**, 489 (1961).
[44] K. Ute, N. Miyatake, and K. Hatada, Polymer **36**, 1415 (1995).
[45] M. Alger, *Polymer Science Dictionary* (Chapman and Hall,

London, 1997), pp. 628.
[46] S. L. Malhotra, L. Minh, and L. P. Blanchard, J. Macromol. Sci., Chem. **A12**, 167 (1978).
[47] G. C. Berry and T. G. Fox, Adv. Polym. Sci. **5**, 261 (1968).
[48] D. J. Plazek, V. Tan, and V. M. O'Rourke, Rheol. Acta **13**, 367 (1974).
[49] B. Jasse, A. K. Oultache, H. Mounach, J. L. Halary, and L. Monnerie, J. Polym. Sci., Part B: Polym. Phys. **34**, 2007 (1996).
[50] K. Fujino, K. Senshu, and H. Kawai, J. Colloid Sci. **16**, 262 (1961).
[51] G. Floudas, J. S. Higgins, F. Kremer, and E. W. Fischer, Macromolecules **25**, 4955 (1992).
[52] D. J. Plazek and V. M. O'Rourke, J. Polym. Sci. A **9**, 209 (1971).